


Xenon and Krypton Dissolved in Water Form Nanoblobs: No Evidence for Nanobubbles

Angela M. Jaramillo-Granada¹, A. D. Reyes-Figueroa^{2,3}, and J. C. Ruiz-Suárez^{1,*}

¹*Centro de Investigación y de Estudios Avanzados-Monterrey, Parque de Investigación e Innovación Tecnológica, 66600 Nuevo León, Mexico*

²*Centro de Investigación en Matemáticas Unidad Monterrey, Av. Alianza Centro No. 502, PIIT, Apodaca, 66628 Nuevo León, Mexico*

³*Consejo Nacional de Ciencia y Tecnología, Av. Insurgentes Sur 1582, Col. Crédito Constructor, Benito Juárez, 03940 CDMX, Mexico*

 (Received 2 December 2021; revised 7 April 2022; accepted 25 July 2022; published 22 August 2022)

We demonstrate, experimentally and by molecular dynamics simulations, that krypton and xenon form nanostructured water-gas domains. High pressure was applied to force the inert gases to dissolve in water following Henry's law, then the liquid was depressurized, centrifuged, and inspected by dynamic light scattering. The observed objects have similar sizes and electrical properties to nanobubbles, but we found that they have fairly neutral buoyancy even at high gravitational fields. We posit that the formed nano objects are not bubbles but blobs, unique structures conceived as clathrate-hydrate precursors, thus resolving the so-called Laplace pressure bubble catastrophe.

DOI: [10.1103/PhysRevLett.129.094501](https://doi.org/10.1103/PhysRevLett.129.094501)

Since the first experimental observation of nanobubbles in 1994 [1], the viability of such enigmatic objects has been supported by numerous research groups that have carried out a vast set of experimental and theoretical studies [2–30]. Nevertheless, despite the overwhelming consensus that nanobubbles are stable and prone to be used as tangible entities in many applications [31–36], there are serious doubts that they exist and are, instead, liquid or solid contaminants [37–42].

The conflicting circumstance is that nanobubbles should not exist because the confined gas, trapped at high pressure (14.5 bar for nanobubbles of radius 100 nm), ought to rapidly escape to the medium [43]. Since their longevities are claimed to be unexpectedly large, the phenomenon has been coined as the Laplace pressure bubble catastrophe [44].

But what if the entities experimentally observed in the labs are neither spurious particles nor nanobubbles? The key point to justify this question is that the gases usually used to presumably form nanobubbles are also capable of being trapped by water cages to give rise to clathrate hydrates. A clathrate hydrate is a water structure that is formed, in three different types, by trapping hydrophobic guest molecules in its interior [45–47]. Moreover, under certain conditions, these structures crystallize into dense ices.

To investigate the possible formation of inert gas nanobubbles with a clean method incapable of creating spurious colloids, we built a novel high-pressure apparatus. Remarkably, while we measured size distributions of entities similar to those found in the nanobubble literature, we also found evidence of dense ices that rapidly (in a few minutes) melted into microscopic surface bubbles, see Fig. S1 in the Supplemental Material [48].

We report in this Letter experimental and molecular dynamics simulations studies that address the nanobubble

puzzling phenomenon. Our findings indicate the feasibility of forming stable krypton and xenon nanodomains that are not recognizable as nanobubbles. Since helium, used as a negative control, was not able to form colloidal particles of any nature following the same experimental protocol, we conclude that the colloids we observe are amorphous clathrate-hydrate nanostructures.

We designed and built a novel pressure apparatus to dissolve inert gases in a given volume of water. A sturdy metallic structure with a fixed hydraulic jack at the bottom was used to support and elevate a platform with a stainless steel cylindrical tube, whose length was 38 cm. The external (internal) diameter of the tube was 3.81 (1.27) cm. A pressure gauge (Instrutek) of 1000 bar and a needle valve (ALCO UN2NS) were attached 5 cm above the bottom at either side of the tube. A stainless steel plunger was fixed to the upper part of the structure. To sustain high gas pressures, we used a rubber stopper (1.4 cm) and a Teflon cylinder (1.28 cm). A thick metallic foil (40 × 25 × 0.5 cm) was fixed in the front part of the structure to provide protection in the event of an explosion, see details in Fig. 1(a).

A glass vial with 2.3 ml of pure Milli-Q water was introduced in the interior of the stainless steel tube, see enlarged frame in Fig. 1(a). The lid of the vial had a small hole of around 300 μm. Then, 9 ml of pure water was poured inside the tube in order to leave the glass vial fully immersed in the water column, which was 5 cm measured from the bottom of the tube. The height of the gas column, from the rubber stopper to the water interface, was 28.8 cm. Through the needle valve, the tube was pressurized with either Kr or Xe gas (with 99% and 99.99% purity, respectively) until a pressure of 15 bar was reached. By means of the hydraulic jack, the platform was raised to

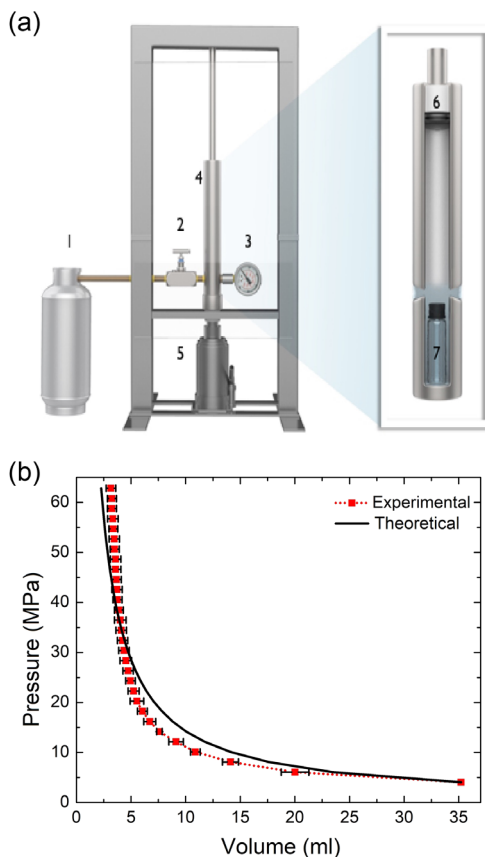


FIG. 1. (a) Schematic of the pressure apparatus. 1. Gas cylinder, 2. needle valve, 3. pressure gauge, 4. stainless steel cylindrical tube, 5. hydraulic jack, 6. rubber stopper, 7. glass vial. (b) P vs V for the ideal gas and experiment ($n = 3$).

reduce the volume of the gas and to augment the pressure, see squares in Fig. 1(b). The P vs V curve follows approximately the ideal gas law $P = nRT/V$, which is very remarkable considering that there is water in the system and the gases dissolve in it. It is important to mention that the rubber stopper approached approximately 1 cm from the water column, indicating that the gas is forced to dissolve in the liquid. The temperature was 25 °C and 60 min were left for equilibration once the required pressure was reached. Depressurization is a crucial step; it was carried out in no less than 30 min. To depressurize, we loosened the hydraulic jack lock so that the tube slowly returned to the original position. The rest of the gas was slowly released through the needle valve. Finally, the vial was taken out from the tube and kept at 4 °C. We waited about two hours until visible bubbles stopped rising by buoyancy. Thereafter, the liquid sample is very stable with no visible bubbles as long as it is handled with care.

Next, dynamic light scattering (DLS) measurements were performed using a zetasizer nano ZSP (Malvern Instruments), see the Supplemental Material for details [48].

In Fig. 2(a) we show the correlograms obtained for Kr and Xe (solid lines), whereas the size distributions (also

solid lines) are depicted in Fig. 2(b). At this stage, as in many other reports, we could assume that we succeeded in forming Kr and Xe nanobubbles. Moreover, since our technique does not employ hydrodynamic or ultrasound cavitation nor organic compounds such as ethanol, we were very confident that contaminants are not produced, see the Supplemental Material and Fig. S3 [48].

Despite the results shown in Figs. 2(a) and 2(b) (solid lines), a decisive proof that we had bubbles would be to get rid of them, so we decided to carry out centrifugation experiments. The glass vials were carefully brought to a swinging-head-type centrifuge (Eppendorf 5804 R) and centrifuged at 4200 G for 2 h. Thereafter, we gently brought the vials back to the DLS apparatus and remeasured the correlograms, see dotted lines in Fig. 2(a). Unexpectedly, they dropped but did not disappear, indicating that the particles were still there. Let us remark that bubbles of ≈ 100 nm subjected to such intense gravitational field would rapidly escape (they will ascend the full height of the vial, 3.4 cm, in 5.6 min), resulting in no correlograms at all. As clearly observed in Fig. 2(b), the size distributions only shifted to smaller sizes.

It is important to point out an interesting situation before continuing. Since centrifugation increases the hydrostatic pressure, gas bubbles must contract. Hence, the possibility exists that contracted bubbles would be so small that buoyancy could be negligible, explaining the results plotted in Figs. 2(a) and 2(b). Thus, a careful analysis is needed to find the change in the radius of the bubbles, see the Supplemental Material and Fig. S4 [48]. We found that, at 4200 G, the contraction of 100 nm nanobubbles is around 20%. Such smaller bubbles must be swept away too in less time than 2 h.

A normal result in the nanobubble literature, confirmed here by our own DLS measurements [see Fig. 2(b)], is that the nanoentities of different gases have radii between 100 and 50 nm. According to the Laplace equation $\Delta P = 2\sigma/r$, where ΔP is the in-out pressure difference and σ is the surface tension, ΔP is between 14.5 and 29 bar. Therefore, considering that the densities of Kr and Xe gases are 3.71 and 5.7 kg/m³ at atmospheric pressure, the gas confined within the nanobubbles would be between 15.5 and 30 times denser: 57.5 and 111.3 for Kr, and 88.35 and 171 kg/m³ for Xe, respectively. In whatever case, even taking into account the correction of the internal pressures modified by centrifugation, the densities are much lower than water's density, so the nanobubbles would be swept away in less than 2 h by a gravitational field like the one we used in this Letter (4200 G). As shown in Fig. 2, this is not the case.

The outcome of the centrifugation experiments gave us an obvious clue: the nanoentities we created are not bubbles but bizarre water-isodense objects. By employing Stokes law, we can calculate the time t a particle lighter (denser) than water will climb (sink) from the bottom (top)

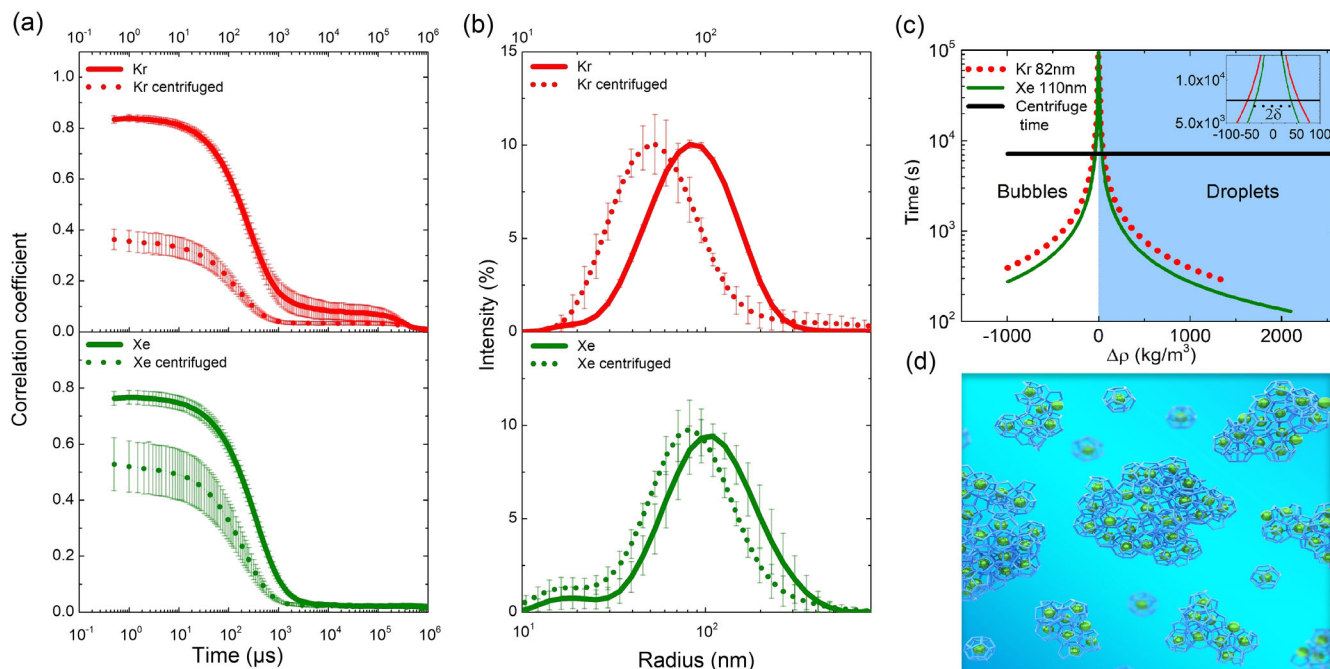


FIG. 2. (a) Correlograms of Kr and Xe nanodomains before and after centrifugation (4200 G, for 2 h). (b) Size distributions of Kr and Xe nanodomains before and after centrifugation (4200 G, for 2 h). At least three experiments were performed, where the shown error bars are standard errors. (c) Residence times of the nanodomains subjected to a gravitational field of 4200 G. (d) Schematic of blob structures.

of the vial of height h : $t = 9h\mu/2gR^2\Delta\rho$, where μ , g , and $\Delta\rho$ are, respectively, the dynamic viscosity of water, gravity, and density difference between particle and water $\rho_p - \rho_w$. Since at this point we do not yet know if the entities we measure by DLS are lighter or denser than water, $\Delta\rho$ can be negative or positive. Figure 2(c) shows t vs $\Delta\rho$ for either case. Clearly, t diverges for $\Delta\rho = 0$. Taking 82 (110) nm as the average radius of the Kr (Xe) specimens we managed to move by centrifugation, we draw the hyperbolic curves shown in Fig. 2(c). The intersections of the horizontal solid line at 7200 s (which is the centrifugation time at 4200 G) with the curves give us the density window $\delta\rho$ around ρ_w of the nanodomains at stake. In other words, the effective density of such domains is $\rho_{\text{eff}} = \rho_w \pm \delta\rho$, with $\rho_w = 998$ and $\delta\rho = 54.3$ kg/m³ for Kr and 38 kg/m³ for Xe.

To conceptually seize the idea that such strange objects exist, we must review the field of clathrate hydrates [45–47,49–54]. A clathrate hydrate is a fused collection of water polyhedral cages that hydrate nonpolar molecules [53]. Kr and Xe are examples of gases that are enclathrated within such polyhedral cavities [52,53,55]. Empty cavities have around 20 water molecules and associate or dissociate in picoseconds, but when a nonpolar molecule is around, it can be trapped by an ephemeral cage gaining stability [52]. Water cages form clathrate hydrates of three different structures (S_1 , S_2 , and S_H). It has been found that Kr and Xe form the first two [52]. Furthermore, at high pressures and low temperatures, clathrate hydrates crystallize into dense

ices. In our experiments, we often found those ices at the bottom of our jars, see Fig. S1 [48].

Interestingly, the most recent theory to account for the formation of clathrate hydrates and ices is based on the existence of amorphous specimens called blobs [45,47,50]. In essence, a blob is an amorphous cluster involving multiple guest molecules in water-mediated configurations [45], see the sketch in Fig. 2(d). As far as we know, blobs have not been observed experimentally, so our guess that we are dealing with them might well come true because we detected them by DLS, but they are, unlike nanobubbles, almost water isodense (a condition easily explained by the water-guest molecules ratio). Moreover, they are not only neutrally buoyant, but are also able to keep their size. Indeed, no coalescence is observed [see Fig. S5(a) in the Supplemental Material [48]], in agreement with their negative charge [Fig. S5(a), inset], and they withstand high temperatures [Fig. S5(b)], in agreement with recent results [56].

Since, according to our centrifugation experiments, the effective density of the blobs is close to water's density, we can estimate the volume fraction ϕ of both Kr and Xe inside them using an effective-medium model [57], see details in the Supplemental Material and Fig. S6 [48]. We found that ϕ_{Kr} and ϕ_{Xe} are, respectively, lower than 0.05 and 0.04. Surprisingly, those volume fractions are on the order of 1/20, a fraction that arises, as above commented, from the fact that each enclathrated guest molecule in a single cage is surrounded by 20 water molecules [49].

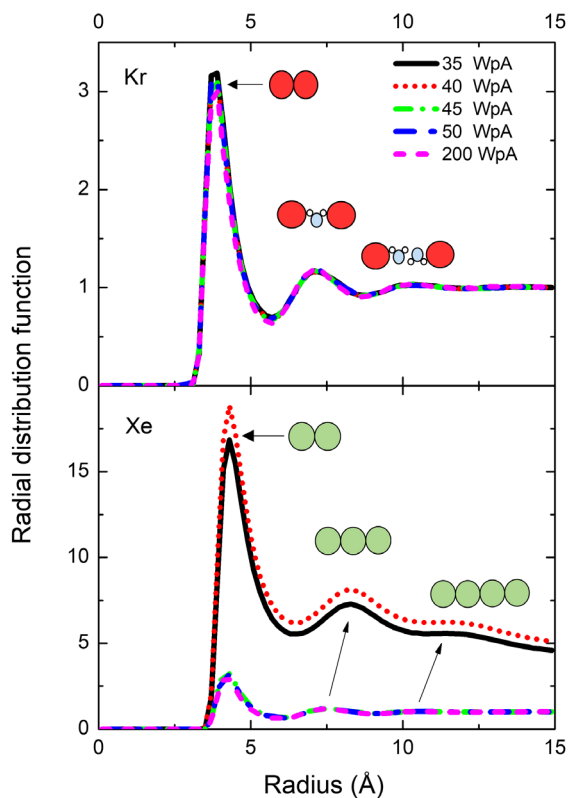


FIG. 3. Radial distribution functions of Kr and Xe obtained by molecular dynamics simulations for various concentrations: 35, 40, 45, 50, and 200 water molecules per guest atom. Note that for Kr all $g(r)$'s match. However, for Xe, the radial distribution functions at 35 and 40 water molecules per atom drastically modify, indicating the emergence of nanobubbles, as observed in Fig. S7 [48]. The peaks in the $g(r)$'s correspond to the events schematically represented in both panels.

We performed molecular dynamics simulations to complement our experiments. Details of the simulations are described in the Supplemental Material [48], as well as in [58–63] and in our recent work [64]. Figure 3 shows radial distribution functions for Kr and Xe for various concentrations. Since the van der Waals radii of the atoms are ≈ 1.8 (Kr) and ≈ 2.0 (Xe) Å, the first peaks correspond to Kr-Kr and Xe-Xe contacts. Next, the second peak in the $g(r)$ of Kr is at 7.02 Å, corresponding to a water molecule, whose van der Waals radius is 1.7 Å [65], between the inert atoms. Finally, the faintly noticeable third peak corresponds to two touching atom-water dimers (10.4 Å). We show the radial distribution functions for Xe at the highest concentrations (35 and 40 water molecules per atom). Clearly, $g(r)$'s suffer great modifications (they increase and shift), indicating that most water molecules are excluded from the domains and Xe clusters and bubbles form, see Fig. S7 [48]. The three peaks correspond now to two, three, and four touching Xe atoms. Regarding this point, it is important to note that the pressure to attain such high Xe concentrations in a real experiment would be around 370 bar, implying that

nanobubbles could exist before depressurization (Laplace pressure does not compromise stability). However, once the cell is depressurized, nanobubbles vanish (as confirmed by our experiments and the radial distribution functions, at lower concentrations, shown in Fig. 3). To illustrate the event, we also depict a snapshot of a zone of the Xe-water diagram for 200 water molecules per Xe atom, see Fig. S8. In order to verify that the observed structures are not affected by the initial configurations, we performed simulations with different initial conditions, see Figs. S9 and S10 in the Supplemental Material [48]. In Fig. S11, we show the time evolution of the Xe clusters formation for the highest concentration (35 water molecules/Xe). Since, at the highest concentrations, Kr bubbles do not form, we did not show their graphs.

Three final points are worth emphasizing before closing: (1) In the literature and in our own experiments, the zeta potentials of “nanobubbles” are negative [see inset of Fig. S5(a)]. Instead of explaining the negative sign based on elaborate suppositions [25,29], it would be easier to consider the restricted orientation of the water molecules at the vertices of the fused cages that form the blobs (where only one hydrogen atom is looking to the bulk, so the negative charge is given by oxygen). (2) The thermal stability of nano-domains observed in Fig. S5(b), and recently reported in [56], would be guaranteed by the endurance of the hydrogen bonds that hold the polyhedral structures together. In this regard, although a theoretical work is needed to explain the stability of the observed nanoentities from the thermodynamic point of view, it is clear that such hydrogen bond interactions strongly reduce enthalpy and, therefore, despite the entropic penalty, free energy. (3) Other authors have previously concluded that nanobubbles, formed by using different techniques, are oily contaminants [38,39,41]. Based on the cleanliness of our method, supported by the negative control experiment done with helium (see Fig. S3), we conclude that the particles we detect are not spurious colloids.

We conclude that Xe and Kr form nanoentities that are not recognizable as nanobubbles. If our findings are extrapolated to other gases like N_2 , CO_2 , and CH_4 , commonly used in the study of nanobubbles but susceptible to form clathrate hydrates and therefore nanostructured domains, there is not Laplace pressure bubble catastrophe to worry about. Physics, then, will not be violated and *ad hoc* models to justify stability will be unnecessary.

This work has been supported by Conacyt, Mexico, under Grants No. FC-1132 and FIDSC-2018 (Grant No. 100). A. M. J.-G. and A. D. R.-F. acknowledge scholarships by Conacyt, Mexico. We thank J. Rafael Guzmán Sepúlveda for helpful discussions, Carlos Samuel Ruiz Vargas for proofreading the manuscript, and David Horta Mendoza for help in the construction of the experimental setup. Computational resources were partly supported by the biophysical systems laboratory of the Universidad Iberoamericana (Puebla).

*Corresponding author.

cruiz@cinvestav.mx

- [1] J. L. Parker, P. M. Claesson, and P. Attard, *J. Phys. Chem.* **98**, 8468 (1994).
- [2] S.-T. Lou, Z.-Q. Ouyang, Y. Zhang, X.-J. Li, J. Hu, M.-Q. Li, and F.-J. Yang, *J. Vac. Sci. Technol. B* **18**, 2573 (2000).
- [3] N. Ishida, T. Inoue, M. Miyahara, and K. Higashitani, *Langmuir* **16**, 6377 (2000).
- [4] K. Kikuchi, H. Takeda, B. Rabolt, T. Okaya, Z. Ogumi, Y. Saihara, and H. Noguchi, *J. Electroanal. Chem.* **506**, 22 (2001).
- [5] R. Steitz, T. Gutberlet, T. Hauss, B. Klösgen, R. Krastev, S. Schemmel, A. C. Simonsen, and G. H. Findenegg, *Langmuir* **19**, 2409 (2003).
- [6] M. Switkes and J. Ruberti, *Appl. Phys. Lett.* **84**, 4759 (2004).
- [7] S. M. Dammer and D. Lohse, *Phys. Rev. Lett.* **96**, 206101 (2006).
- [8] L. Zhang, Y. Zhang, X. Zhang, Z. Li, G. Shen, M. Ye, C. Fan, H. Fang, and J. Hu, *Langmuir* **22**, 8109 (2006).
- [9] J. Martinez and P. Stroeve, *J. Phys. Chem. B* **111**, 14069 (2007).
- [10] H. Seo, M. Yoo, and S. Jeon, *Langmuir* **23**, 1623 (2007).
- [11] X. H. Zhang, A. Khan, and W. A. Ducker, *Phys. Rev. Lett.* **98**, 136101 (2007).
- [12] X. H. Zhang, A. Quinn, and W. A. Ducker, *Langmuir* **24**, 4756 (2008).
- [13] L. Zhang, H. Chen, Z. Li, H. Fang, and J. Hu, *Sci. China Ser. G* **51**, 219 (2008).
- [14] Z. Wu, H. Chen, Y. Dong, H. Mao, J. Sun, S. Chen, V. S. Craig, and J. Hu, *J. Colloid Interface Sci.* **328**, 10 (2008).
- [15] W. A. Ducker, *Langmuir* **25**, 8907 (2009).
- [16] K. Ohgaki, N. Q. Khanh, Y. Joden, A. Tsuji, and T. Nakagawa, *Chem. Eng. Sci.* **65**, 1296 (2010).
- [17] V. S. J. Craig, *Soft Matter* **7**, 40 (2011).
- [18] J. R. T. Seddon, H. J. W. Zandvliet, and D. Lohse, *Phys. Rev. Lett.* **107**, 116101 (2011).
- [19] S. Karpitschka, E. Dietrich, J. R. T. Seddon, H. J. W. Zandvliet, D. Lohse, and H. Riegler, *Phys. Rev. Lett.* **109**, 066102 (2012).
- [20] C. U. Chan and C.-D. Ohl, *Phys. Rev. Lett.* **109**, 174501 (2012).
- [21] L. Luo and H. S. White, *Langmuir* **29**, 11169 (2013).
- [22] L. Zhang, B. Zhao, L. Xue, Z. Guo, Y. Dong, H. Fang, R. Tai, and J. Hu, *J. Synchrotron Radiat.* **20**, 413 (2013).
- [23] X. Zhang, D. Y. Chan, D. Wang, and N. Maeda, *Langmuir* **29**, 1017 (2013).
- [24] D. Lohse, X. Zhang *et al.*, *Rev. Mod. Phys.* **87**, 981 (2015).
- [25] N. Nirmalkar, A. Patek, and M. Barigou, *Langmuir* **34**, 10964 (2018).
- [26] S. Ke, W. Xiao, N. Quan, Y. Dong, L. Zhang, and J. Hu, *Langmuir* **35**, 5250 (2019).
- [27] A. J. Jadhav and M. Barigou, *Langmuir* **36**, 1699 (2020).
- [28] G. Ferraro, A. J. Jadhav, and M. Barigou, *Nanoscale* **12**, 15869 (2020).
- [29] B. H. Tan, H. An, and C.-D. Ohl, *Phys. Rev. Lett.* **124**, 134503 (2020).
- [30] L. Zhou, X. Wang, H.-J. Shin, J. Wang, R. Tai, X. Zhang, H. Fang, W. Xiao, L. Wang, C. Wang *et al.*, *J. Am. Chem. Soc.* **142**, 5583 (2020).
- [31] A. Agarwal, W. J. Ng, and Y. Liu, *Chemosphere* **84**, 1175 (2011).
- [32] A. Ushida, T. Hasegawa, T. Nakajima, H. Uchiyama, and T. Narumi, *Exp. Therm. Fluid. Sci.* **39**, 54 (2012).
- [33] N. Matsuki, T. Ishikawa, S. Ichiba, N. Shiba, Y. Ujike, and T. Yamaguchi, *Int. J. Nanomed.* **9**, 4495 (2014).
- [34] A. Roy, K. K. Modi, S. Khasnavis, S. Ghosh, R. Watson, and K. Pahan, *PLoS One* **9**, e101883 (2014).
- [35] A. Ghadimkhani, W. Zhang, and T. Marhaba, *Chemosphere* **146**, 379 (2016).
- [36] S. Liu, S. Oshita, Y. Makino, Q. Wang, Y. Kawagoe, and T. Uchida, *ACS Sustainable Chem. Eng.* **4**, 1347 (2016).
- [37] A. Hbich, W. Ducker, D. E. Dunstan, and X. Zhang, *J. Phys. Chem. B* **114**, 6962 (2010).
- [38] M. Sedlák and D. Rak, *J. Phys. Chem. B* **117**, 2495 (2013).
- [39] M. Alheshibri and V. S. Craig, *J. Phys. Chem. C* **122**, 21998 (2018).
- [40] D. Rak, M. Ovadová, and M. Sedlák, *J. Phys. Chem. Lett.* **10**, 4215 (2019).
- [41] M. Alheshibri and V. S. Craig, *J. Colloid Interface Sci.* **542**, 136 (2019).
- [42] D. Rak and M. Sedlák, *Langmuir* **36**, 15618 (2020).
- [43] F. Lugli, S. Höfner, and F. Zerbetto, *J. Am. Chem. Soc.* **127**, 8020 (2005).
- [44] M. Alheshibri, J. Qian, M. Jehannin, and V. S. Craig, *Langmuir* **32**, 11086 (2016).
- [45] L. C. Jacobson, W. Hujo, and V. Molinero, *J. Am. Chem. Soc.* **132**, 11806 (2010).
- [46] S. Mondal and P. K. Chattaraj, *Phys. Chem. Chem. Phys.* **16**, 17943 (2014).
- [47] M. Khurana, Z. Yin, and P. Linga, *ACS Sustainable Chem. Eng.* **5**, 11176 (2017).
- [48] See Supplemental Material at <http://link.aps.org/supplemental/10.1103/PhysRevLett.129.094501> for more experimental results, discussion, and details of our molecular dynamics simulations.
- [49] V. I. Artyukhov, A. Y. Pulver, A. Peregudov, and I. Artyuhov, *J. Chem. Phys.* **141**, 034503 (2014).
- [50] N. J. English, M. Lauricella, and S. Meloni, *J. Chem. Phys.* **140**, 204714 (2014).
- [51] P. Teeratchanan and A. Hermann, *J. Chem. Phys.* **143**, 154507 (2015).
- [52] H. Tanaka, T. Yagasaki, and M. Matsumoto, *J. Chem. Phys.* **149**, 074502 (2018).
- [53] S. P. Kaur and C. Ramachandran, *Mol. Phys.* **116**, 54 (2018).
- [54] R. Yanes-Rodríguez and R. Prosmitti, *Phys. Chem. Chem. Phys.* **24**, 1475 (2022).
- [55] A. Rasoolzadeh, L. Aaldijk, S. Raeissi, A. Shariati, and C. J. Peters, *Fluid Phase Equilib.* **512**, 112528 (2020).
- [56] M. Li, X. Ma, J. Eisener, P. Pfeiffer, C.-D. Ohl, and C. Sun, *J. Colloid Interface Sci.* **596**, 184 (2021).
- [57] L. Gibilaro, K. Gallucci, R. Di Felice, and P. Pagliai, *Chem. Eng. Sci.* **62**, 294 (2007).
- [58] H. J. C. Berendsen, J. P. M. Postma, W. F. van Gunsteren, and J. Hermans, in *The Jerusalem Symposia on Quantum Chemistry and Biochemistry* (Springer, Netherlands, 1981), pp. 331–342.

- [59] G. Rutkai, M. Thol, R. Span, and J. Vrabec, *Mol. Phys.* **115**, 1104 (2017).
- [60] S. Nosé, *Mol. Phys.* **52**, 255 (1984).
- [61] W. G. Hoover, *Phys. Rev. A* **31**, 1695 (1985).
- [62] M. Parrinello and A. Rahman, *J. Appl. Phys.* **52**, 7182 (1981).
- [63] M. J. Abraham, T. Murtola, R. Schulz, S. Páll, J. C. Smith, B. Hess, and E. Lindahl, *SoftwareX* **1**, 19 (2015).
- [64] A. Reyes-Figueroa, M. Karttunen, and J. Ruiz-Suárez, *Soft Matter* **16**, 9655 (2020).
- [65] A.-J. Li and R. Nussinov, *Proteins* **32**, 111 (1998).